



## MECHANICAL PROPERTIES OF MARTENSITIC PRECIPITATION HARDENED STAINLESS STEEL PRODUCED BY SELECTIVE LASER MELTING

Mohamed A. Elsharkawy<sup>1,\*</sup>, Mohamed Bayoumi<sup>2</sup>, Khalid Abdelghany<sup>1</sup>, Haytham Elgazzar<sup>1</sup>

<sup>1</sup> Advanced Digital Manufacturing Department, Central Metallurgical Research and Development Institute (CMRDI), Cairo, Egypt.

<sup>2</sup> Department of Mechanical Engineering, Faculty of Engineering, Al-Azhar University, Cairo, Egypt.

\* Correspondence: [mohamedelsharkawy070@gmail.com](mailto:mohamedelsharkawy070@gmail.com)

### Citation:

M. A. Elsharkawy, M. Bayoumi, K. Abdelghany and H. Elgazzar, "Mechanical properties of martensitic precipitation hardened stainless steel produced by selective laser melting", Journal of Al-Azhar University Engineering Sector, Vol. 19, pp. 88 - 100, 2024.

Received: 7 September 2023

Revised: 2 November 2023

Accepted: 19 November 2023

DOI: 10.21608/aej.2023.234835.1415

Copyright © 2024 by the authors. This article is an open-access article distributed under the terms and conditions of Creative Commons Attribution-Share Alike 4.0 International Public License (CC BY-SA 4.0)

### ABSTRACT

Martensitic precipitation hardened stainless steel, of which 17-4PH stainless steel is the most common, is used in various industrial fields due to its high strength and excellent corrosion resistance. The selective laser melting (SLM) technique can produce complicated components using lower material quantities and fewer steps compared to traditional manufacturing methods. The aim of this paper is to study the influence of SLM processing parameters, mainly laser power, scanning speed, and hatching space (percent of overlapping), on the density, micro-hardness, and tensile strength of 17-4PH stainless steel.

The study showed that higher densities as well as higher tensile strength can be obtained by increasing the laser power or decreasing the scanning speed, taking into account the production time. The optimal laser power and scanning speed range are 150–200 watts and 200–400 mm/sec, respectively. The best constant layer thickness is 50  $\mu\text{m}$ , and the laser spot diameter is 150  $\mu\text{m}$ . A correlation between the mechanical properties of the produced specimens and the prevailing process parameters has also been established.

**KEYWORDS:** Additive manufacturing, Selective laser melting (SLM), 17-4PH stainless steel, Tensile strength, Micro-hardness.

### دراسة الخواص الميكانيكية للصلب المقاوم للصدأ المصنوع باستخدام تقنية الصهر الانتقائي بالليزر

محمد عبد اللطيف الشراقوي<sup>1,\*</sup>، محمد بيومي<sup>2</sup>، خالد عبد الغني<sup>1</sup>، هيثم الجزار<sup>1</sup>

<sup>1</sup> قسم التصنيع الرقمي المتقدم، مركز بحوث وتطوير الفلزات، القاهرة، مصر

<sup>2</sup> قسم الهندسة الميكانيكية، كلية الهندسة، جامعة الأزهر، القاهرة، مصر

\* البريد الإلكتروني للباحث الرئيسي: [mohamedelsharkawy070@gmail.com](mailto:mohamedelsharkawy070@gmail.com)

### الملخص

يستخدم الصلب المقاوم للصدأ 17-4 PH في العديد من التطبيقات نظراً لتميزه بمتانة الشد العالية ومقاومته للتآكل. تتميز عملية التصنيع باستخدام الطباعة ثلاثية الأبعاد بإنتاج منتجات ذات أشكال معقدة يصعب إنتاجها بطرق التصنيع التقليدية حيث يتم بناء المنتجات بإضافة طبقة تلو الأخرى من المادة إلى أن يتم الانتهاء من المنتج على عكس طرق التصنيع التي تعتمد على تشغيل المواد عن طريق إزالة جزء من المادة بواسطة أدوات القطع. الهدف من هذه الدراسة هو تقييم استخدام تكنولوجيا الطباعة ثلاثية الأبعاد لإنتاج منتجات من الصلب المقاوم للصدأ 17-4 PH، بالإضافة إلى ذلك توصيف خصائص المنتجات الميكانيكية (الشد و الصلادة) المصنعة بهذه الطريقة.

تم دراسة تأثير كل من قدرة الليزر وسرعة المسح ونسبة التداخل بين مسارات الليزر المتتالية على الخواص الميكانيكية للأجزاء المصنعة

تظهر الدراسة أن القيم المثلى لكثافة العينات وخصائصها الميكانيكية تتحقق مع زيادة قدرة الليزر أو تقليل سرعة المسح بالليزر، كما يؤخذ في الاعتبار زمن بناء العينات. حيث تبين الدراسة أن القيم المثلى لقدرة الليزر ما بين 150 الى 200 وات و لسرعة المسح بالليزر ما بين 200 الى 400 ملليميتر لكل ثانية وذلك عند سمك 50 ميكروميتر لكل طبقة و قطر بؤرة شعاع الليزر 150 ميكروميتر .

**الكلمات المفتاحية:** الصلب المقاوم للصدأ 17-4PH ، الطباعة ثلاثية الأبعاد، تقنية الصهر الانتقائي بالليزر، مقاومة الشد، الصلادة.

## 1. INTRODUCTION

Additive manufacturing (AM) has a great interest in many industries, including the biomedical, automotive, and aerospace sectors. Additive manufacturing (AM), a 3D printing technique, is based on consecutive layer processing based on slicing process output data based on a 3D CAD model.

Selective laser melting (SLM), an additive manufacturing process, can produce 3D metallic parts using different powders as raw materials by selectively melting stacked layers of powder by a galvo-guided laser focused beam, where a layer's cross section is scanned by a laser beam, then the building platform is lowered, the powder platform is raised, and a new powder layer is deposited, as shown in **Fig. 1**. This process is iterated until the part is built. Unlike traditional machining, turning, and milling processes, where material is removed from a stock item. SLM enables the production of complex shapes using less material than traditional manufacturing methods [1].

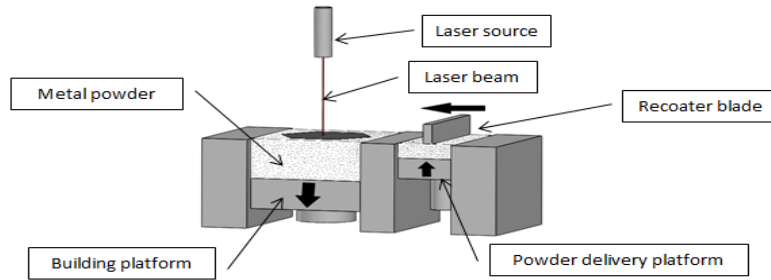


**Fig. 1:** Sketch of Selective Laser Melting processing.

Laser power, scanning speed, hatching space, layer thickness, scanning strategy, and building orientation are the prevailing parameters that influence the final quality of the SLM-processed specimens. In this study, laser power, scanning speed, and hatching space of the following magnitudes are investigated with the following values: 50-200 watts, 200-1000 mm/sec, and 20-120  $\mu\text{m}$ , respectively, while the other parameters were kept constant.

Laser power, scanning speed, layer thickness, and laser spot diameter have a direct effect on the laser heat input. The laser heat energy input manipulates the level of consolidation of the powder particulates or could potentially initiate defects via turbulence in the molten steel pool that can lead to a keyhole defect in the resonant conditions.

The energy density  $\Psi$  can be used as an index of the total heat energy input implied by the laser source.

$$\Psi = \frac{4P}{v \cdot t \cdot \pi D^2} \quad \text{J/mm}^3 \quad \text{Eq. 1 [2]}$$

Where,

- $P$  laser power (Watts),
- $v$  scanning speed (mm/s),
- $t$  layer thickness (mm), and
- $D$  laser spot diameter (mm).

Thus, the laser power, scanning speed, and layer thickness can be controlled during the selective melting process.

According to Eq. 1, insufficient laser power or a faster than required scanning speed would imply a low energy density, which leads to incomplete melting and, hence, a very porous product. An excessive energy density (i.e., extreme laser power and low scanning speed) can cause an excessive melting pool, hence creating balling defects and a higher pore rate [3].

It can be observed that at insufficient energy density, the part density drops (porosity increases) due to incomplete fusion. The part density might also drop at excessive energy density due to keyhole defects being formed as a result of enclosed metal vapor within an excessive melting pool. Appropriate energy density may produce sound parts with acceptable properties. The value of the appropriate energy density depends on the type of material and the machine [3].

It has been mentioned that the yield strength and ultimate tensile strength increase when increasing laser power or decreasing scanning speed [4]. It has been shown that the ultimate tensile strength and elongation of the SLM-processed specimens were greater than those of the wrought specimens. On the other side, the yield strength of the SLM-processed specimens was less than that of the wrought specimens [5, 6]. It has been mentioned that the yield strength of the SLM-processed 17-4PH stainless steel slightly dropped in comparison to the wrought alloy [7].

The effects of normal, concentric, and hexagonal scanning strategies have been studied; specimens that are normally and hexagonally scanned exhibit similar tensile behavior, with an ultimate tensile strength of about 1100 MPa and a yield strength of about 712 MPa. However, the concentric strategy displayed more ductile behavior [8]. The influence of building orientation on the tensile properties of SLM-processed 17-4PH stainless steel has been studied. The studies indicate that vertically fabricated specimens exhibit lower yield, and ultimate tensile strength, and elongation to failure than horizontally fabricated specimens. It has also been mentioned that the yield and ultimate tensile strength of the SLM-processed 17-4 PH stainless steel specimens dropped in comparison to the wrought materials [9, 10].

It has been found that increasing laser power causes an increase in microhardness [4, 5]. It has been mentioned that the micro-hardness decreases with increasing scanning speed [4, 11, 12]. It has been found that the average micro-hardness values are close to 310 HV [13]. It has been mentioned that the concentric strategy has lower hardness than the normal and hexagonal strategies [8]. The influence of scanning strategies (hexagonal vs. concentric) on the hardness of 17-4PH stainless steel specimens was investigated. It has been found that the average hardness of fabricated specimens using the hexagon scanning strategy was about 11% higher than that of those produced using the concentric strategy [14].

The present research aims to study the influence of SLM processing parameters on the density, micro-hardness, and tensile strength of 17- 4PH stainless steel. A correlation between the mechanical properties of specimens and the processing parameters has been established.

## 2. Experimental work

### 2.1. Material

17-4 PH stainless steel powder (CL92PH stainless steel powder) with a diameter between 15 and 45  $\mu\text{m}$  supplied by TIGO METAL MATERIAL CO., Changsha City, China, is used in this investigation. The chemical composition of the powder that was analyzed in the CMRDI chemical test lab using a Niton XL3t XRF analyzer is shown in Table 1. The mechanical and physical properties of the wrought 17-4PH stainless steel (ASTM A693 hot-rolled plates) are shown in Table 2.

**Table 1:** Powder 17-4PH stainless steel chemical composition.

Chemical composition (wt.%)										
Cr	Ni	Cu	Si	Mn	C	Nb	S	P	Mo	Fe
17.007	4.33	4.205	0.271	0.776	0.022	0.4	0.011	0.008	0.048	72.2

**Table 2:** The wrought 17-4PH stainless steel mechanical and physical properties (ASTM A693 hot rolled plates), Sandmeyer Steel Company, United States, Pennsylvania.

Mean mechanical properties				
Ultimate tensile strength (MPa)	Yield strength (MPa)	Elongation (%)	Hardness (HV)	
965-1034	790-931	10-17	349	
Physical properties				
Melting range °C	Density ( $g/cm^3$ )	Modulus of Elasticity (GPa)	Specific Heat J/kg-°C @ 20°C	Thermal Conductivity (W/m.k)
1404–1440	7.75	196	460	18.4

### 2.1.1. Equipment

17-4PH stainless steel specimens have been fabricated using a CONCEPT Laser, an M3 Linear machine, equipped with a Nd: YAG 200W Solid-state laser located in the Advanced Digital Manufacturing Department, CMRDI, Egypt. Further details of this machine are shown in the following Table 3. The process was carried out in a high purity Nitrogen ( $N_2$ ) gas atmosphere. EDM Wire Cut was used to remove the fabricated specimens from the building plate.

**Table 3:** The specifications of the machine

Positioning precision of the linear motors	15 $\mu$ m
Build plate	250 x 250 x 250 mm
Layer thickness	20 - 80 $\mu$ m
Weight of workpiece	up to 500 kg
Laser system	Nd:YAG Solid state laser 200W Wavelength 1.064 $\mu$ m
Max. scanning speed	7 m/sec
Spot diameter	150 $\mu$ m
Inert gas supply	N2 generator external

## 2.2. Manufacturing and mechanical properties investigation

### 2.2.1. Specimen preparation and the preliminary experiments

The experiments, tensile test specimens, as shown in Fig. 2, were carried out in two stages: preliminary and final experiments. A set of preliminary experiments was done to reach the appropriate processing parameters for the final experiments. The process was performed using the island scanning strategy (5 mm x 5 mm) under a high purity nitrogen ( $N_2$ ) gas atmosphere with a constant layer thickness of 50  $\mu$ m and a 150  $\mu$ m laser spot diameter.

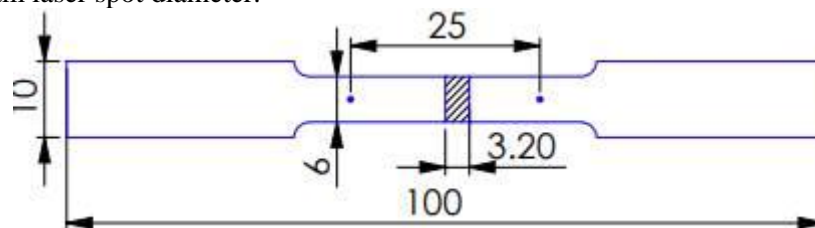


**Fig. 2:** Dimensions of tensile test specimen that used in the experiments

The preliminary experiment parameters are listed in Table 4.

**Table 4:** A set of preliminary experiments to select the area of the final experiments at different laser powers ( $P$ ), scanning speeds ( $v$ ), and hatching spaces ( $h$ )

Specimen No.	$P$ (Watts)	$v$ (mm/sec)	Overlap ( $h$ ( $\mu\text{m}$ ))
1	50	200	60 (60)
2	100	200	60 (60)
3	150	200	60 (60)
4	200	200	60 (60)
5	200	400	60 (60)
6	200	600	60 (60)
7	200	800	60 (60)
8	200	1000	60 (60)
9	200	1200	60 (60)
10	200	100	60 (60)
11	200	600	80 (30)
12	200	600	40 (90)
13	200	600	20 (120)

Thirteen tensile specimens have been produced through the preliminary experiment to find out the status of the produced specimens, that is, the completed/incompleted ones. Completely printed specimens were characterized accurately to reach the optimal ranges of laser powers and scanning speeds. Specimens from 1 to 4, specimens from 4 to 10, and specimens 6, 11, 12, and 13 were performed to select the optimal laser powers, scanning speeds, and hatching space values, respectively.

The relative density, elongation, yield, and ultimate strength are measured for the completely SLM-processed specimens from preliminary experiments. The specimen's density was measured using the Archimedes method. The porosity was also detected using optical microscopy (cell Sens Entry software, OLYMPUS PMG 3, Japan). Using the walter+bai testing machine (20 KN), tension force was applied to each specimen with a test speed of 5 mm/min to obtain the stress-strain diagram of each specimen. From this diagram, yield strength, ultimate strength, and elongation were obtained.

### 2.2.2. The final experiments

From the results obtained from the preliminary experiments, it has been decided to carry out the final experiments, where the following processing parameters have been used: laser powers (150 and 200 watts), scanning speeds (200 and 400 mm/min), and hatching spaces (60 and 90  $\mu\text{m}$ ).

The relative density, micro-hardness, elongation, yield, and ultimate strength were measured for the final experiment specimens to select the optimum laser power, scanning speed, and hatching space.

The micro-hardness on the top and side surfaces of a specimen of dimensions 10 x 10 x 10  $\text{mm}^3$  (as shown in **Fig. 3**) was measured. Ten tests' points at intervals of 250  $\mu\text{m}$  along one direction are conducted by the SHIMADZU Micro Hardness Tester with a 100 g load for 30 seconds.

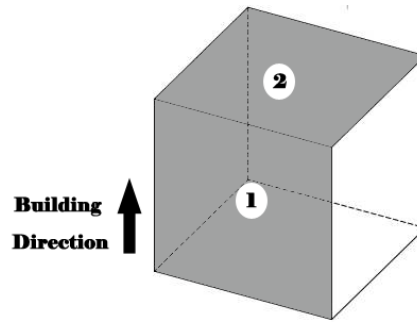


**Fig. 3:** The area of micro-hardness measurements (1) Side surface (2) Top surface.

### 3. Results and discussion

#### 3.1. The preliminary experiment results

A set of preliminary experiments was done to determine the best area for the final experiments. Table 5 lists the SLM-processed building status at different laser powers and scanning speeds with constant hatching space (60  $\mu\text{m}$ ).

**Table 5:** SLMed building status at different laser powers and scanning speeds (at hatching space = 60  $\mu\text{m}$ )

Specimen No.	$P$ (Watts)	$v$ (mm/sec)	Building status
1	50	200	Incomplete
2	100	200	Completed
3	150	200	Completed
4	200	200	Completed
5	200	400	Completed
6	200	600	Completed
7	200	800	Completed
8	200	1000	Completed
9	200	1200	Incomplete
10	200	100	Over-heating

At specimens' numbers 1 and 9 at laser power, and scanning speed (50,200), and (200,1200), respectively, there is insufficient heat energy that led to an incomplete building, as shown in Fig. 4.

Therefore, it is evident that values of laser power and scanning speed less than those values cannot result in a complete building. Fig. 5 shows the zone of the processing parameters that can be used to produce a complete building. Fig. 6 shows the complete build of the SLM-processed specimen.



**Fig. 4:** Incompletely building at laser power 50 watts and scanning speed 200 mm/sec

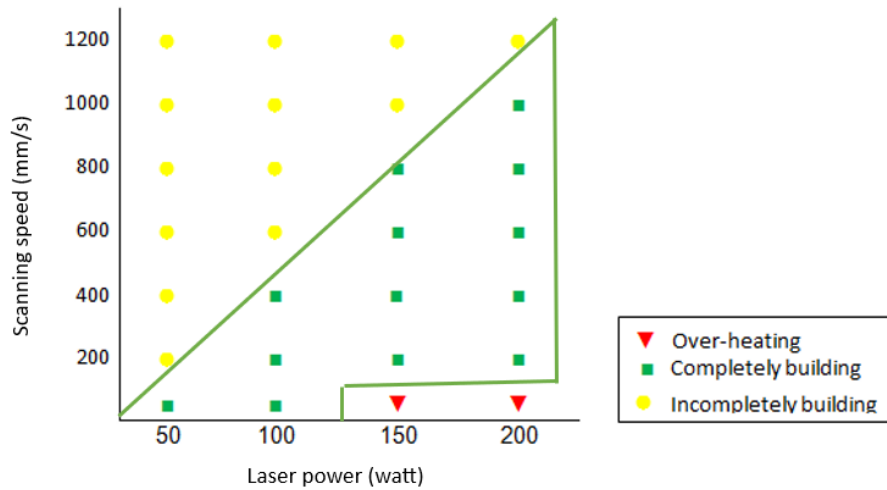


Fig. 5: The preliminary experiments to select a completely SLMed building

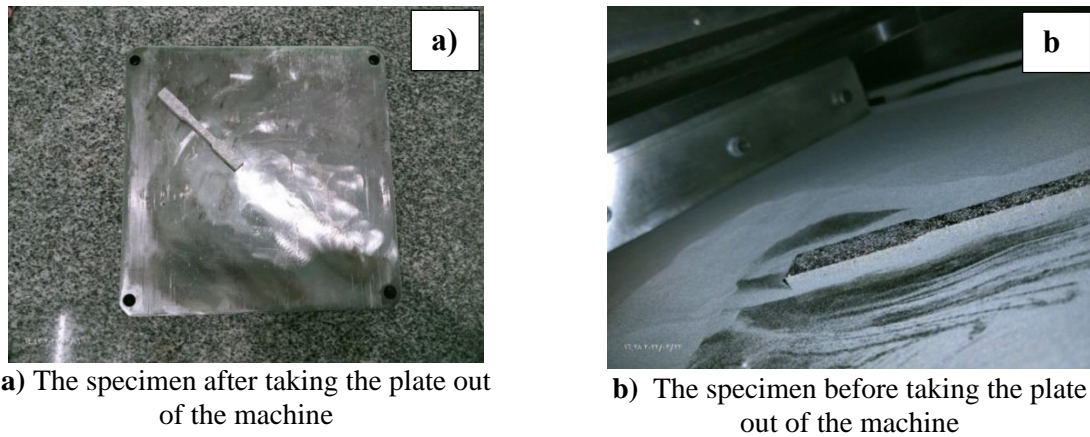


Fig. 6: SLMed tensile test specimen

### 3.1.1. The effect of laser power and scanning speed on the density and mechanical properties

Fig. 7 shows the effect of laser power on the relative density compared to theoretical TD%, yield strength, and ultimate tensile strength measured for the completed SLM -processed specimens with a scanning speed of 200 mm/sec, hatching space of 60  $\mu\text{m}$ , and a constant layer thickness of 50  $\mu\text{m}$ . While Fig. 8 shows the effect of scanning speed on those characteristics with a laser power of 200 watts, a hatching space of 60  $\mu\text{m}$ , and a constant layer thickness of 50  $\mu\text{m}$ .

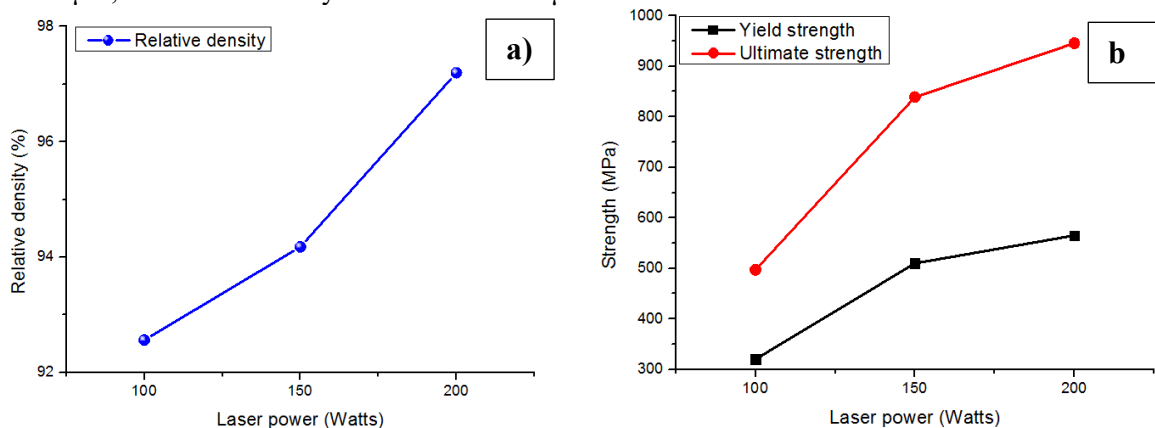
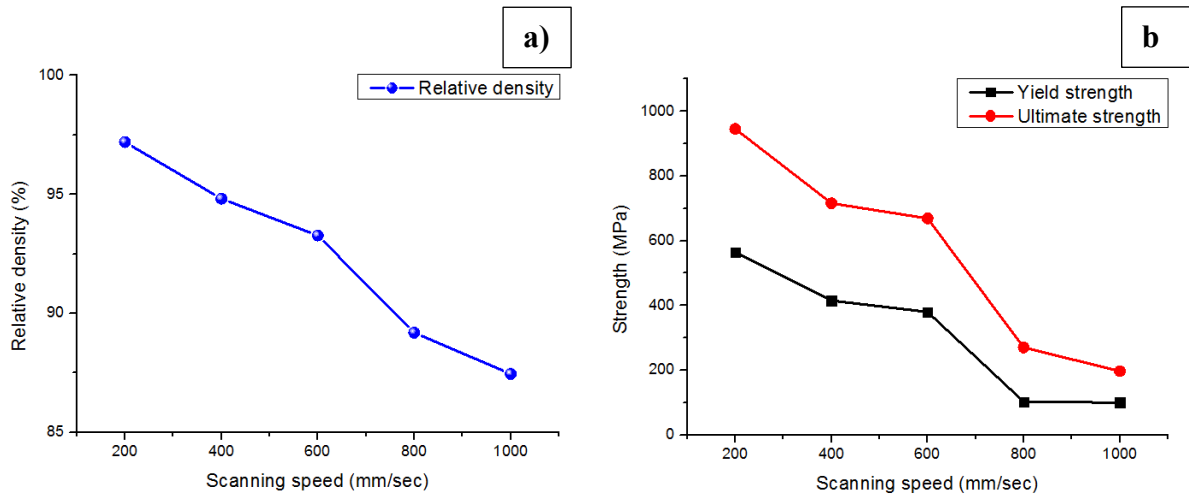


Fig. 7: Effect of laser power on a) relative density, b) yield and ultimate. strength (scanning speed 200 mm/sec, hatching space 60  $\mu\text{m}$ )



**Fig. 8:** Effect of scanning speed on a) relative density, b) yield and ultimate strength (laser power 200 watts, hatching space 60  $\mu\text{m}$ )

It can be noted that laser power and scanning speed are decisive factors that partly manipulate density, yield strength, and ultimate tensile strength. Increasing laser power would lead to higher density, yield strength, and ultimate tensile strength of the SLM-processed specimens. Fig. 9 shows relative porosity with a magnification of  $100\times$  using different laser powers. It can be seen that when laser power decreases, the energy input is insufficient, so the powder is incompletely melted, leading to more porosity, as shown in Fig. 9 (a). Appropriate energy input leads to nearly complete fusion, i.e., lower porosity, as shown in Fig. 9 (b).

Increasing scanning speed leads to lower density, yield strength, and ultimate tensile strength of specimens. As scanning speed increases above 200 mm/s, the energy input is insufficient, so the powder is incompletely melted, leading to multiple porosities due to the lower wettability of the molten metal pool. Therefore, large and complex porosities form, as shown in Fig. 10 (b). When the scanning speed is about 200 mm/sec, material evaporates less frequently, and the formation of shielding gas porosity will be reduced. Accordingly, defects decrease, as shown in Fig. 10 (a). As scanning speed decreases below 200 mm/sec, laser energy input is so excessive that material is extensively evaporated, forming gaseous bubbles.

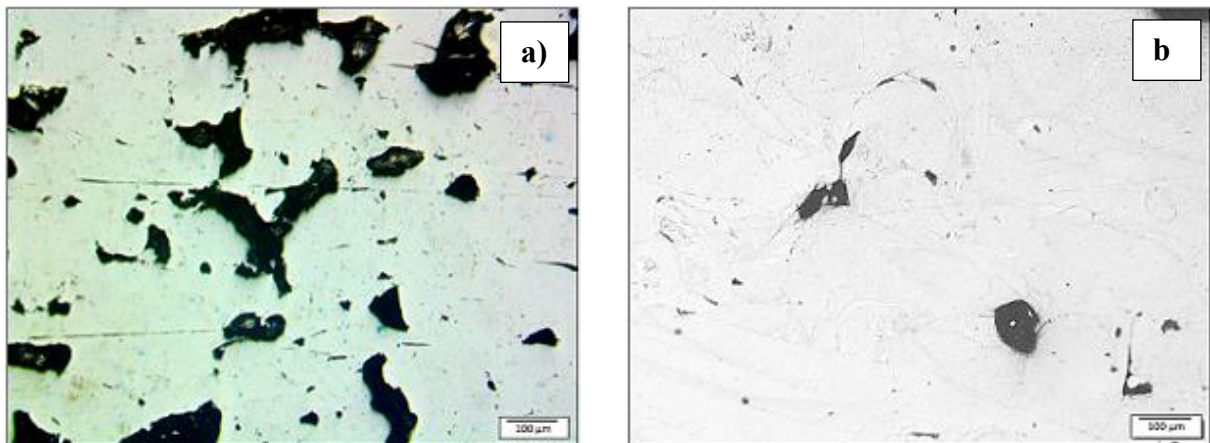


**Fig. 9:** The porosity percentage with a magnification of  $100\times$  using different laser power a) 100 watts and b) 200 watts at a scanning speed of 200 mm/sec and a hatching space of 60  $\mu\text{m}$



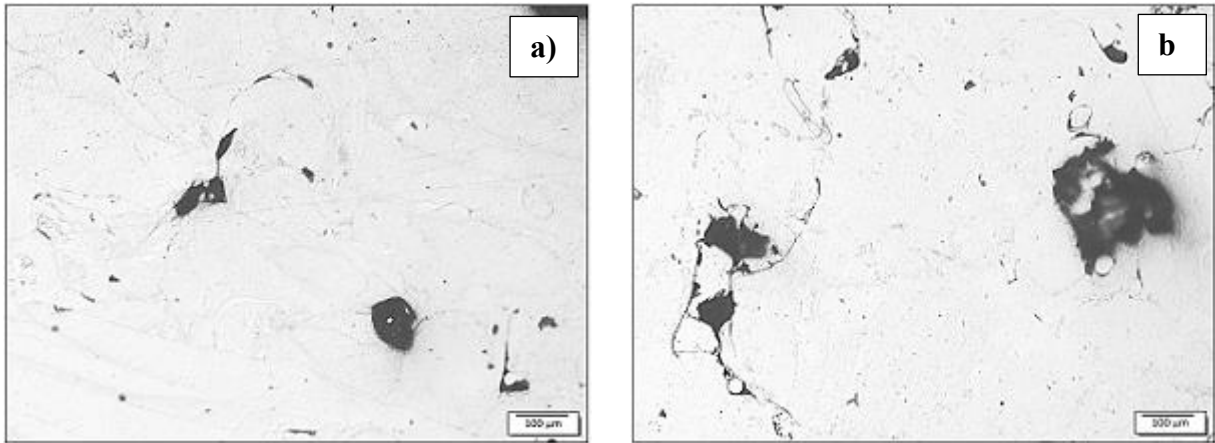


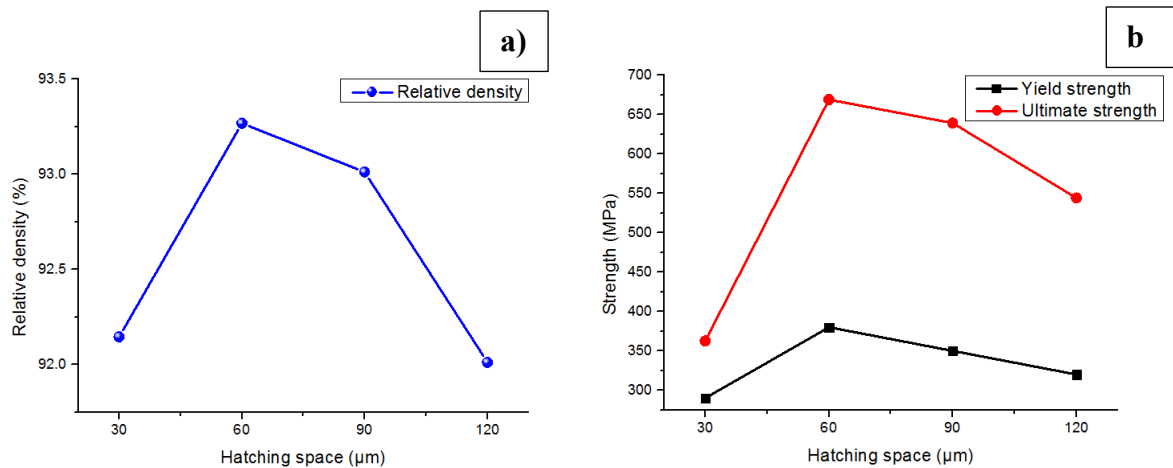
**Fig. 10:** The porosity percentage with a magnification of  $100_x$  using different scanning speed a) 200 mm/sec and b) 600 mm/sec at a laser power of 200 watts and a hatching space of 60 μm

### 3.1.2. The effect of hatching space on the density and mechanical properties

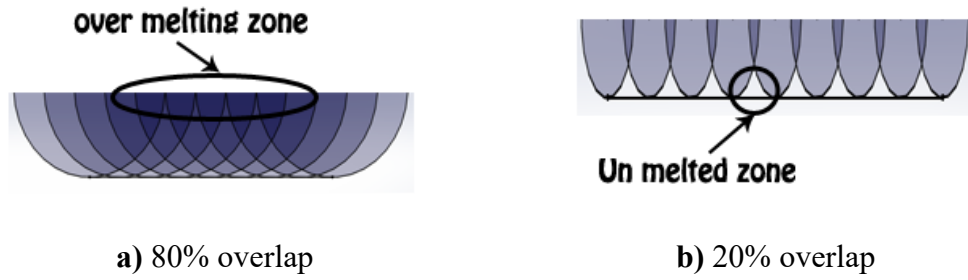
The effect of hatching space on relative density, yield strength, and ultimate tensile strength was also studied. The SLM process was conducted using a laser power of 200 watts and a scanning speed of 600 mm/sec under the protective atmosphere of a high purity nitrogen gas. Tensile test specimens were fabricated at different overlap values (20 %, 40%, 60%, 80%).

Fig. 11 shows that in specimens numbers 11 and 13 with overlap of 80% and 20%, respectively, the relative densities, yield strengths, and ultimate tensile strengths of specimens are lower than in specimens' numbers 6 and 12 with overlap of 60% and 40%, respectively. This may be attributed to the entrapped metal vapor inside the molten pool for 80% overlap and due to incomplete melting at 20% overlap, as explained schematically in Fig. 12. The specimens with 60% and 40% overlaps have higher densities and mechanical properties because they have lower porosity percentages, as shown in Fig. 13.

So, the suitable overlap values for investigation are 40% and 60% due to the highest density, yield strength, and ultimate tensile strength values.



**Fig. 11:** Effect of hatching space on a) relative density, b) yield and ultimate strength (laser power 200 watts, scanning speed 600 mm/sec)



**Fig. 12:** The overlapping model schematic

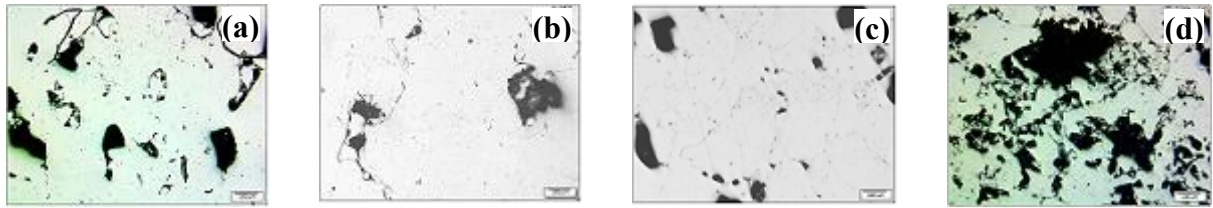


**Fig. 13:** The porosity percentage with a magnification of  $100_x$  using different overlap (a) 80%, (b) 60%, (c) 40%, and (d) 20% at a scanning speed of 200 mm/sec and a laser power of 200 watts

After reviewing the preliminary experiments, it can be said that the experiments that can be investigated to reach the best results are as follows in Table 6.

**Table 6:** The processing parameters for final experiments

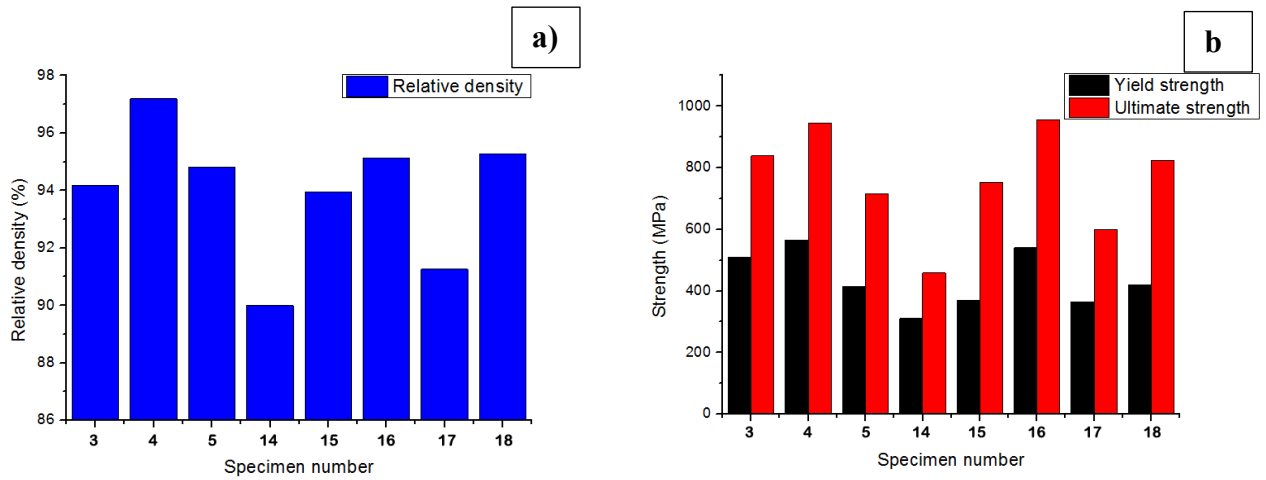
Specimen No.	$P$ (Watts)	$v$ (mm/sec)	Overlap ( $h$ ( $\mu\text{m}$ ))
3	150	200	60(60)
4	200	200	60(60)
14	150	400	60(60)
5	200	400	60(60)
15	150	200	40(90)
16	200	200	40(90)
17	150	400	40(90)
18	200	400	40(90)

### 3.2. The final experiment results

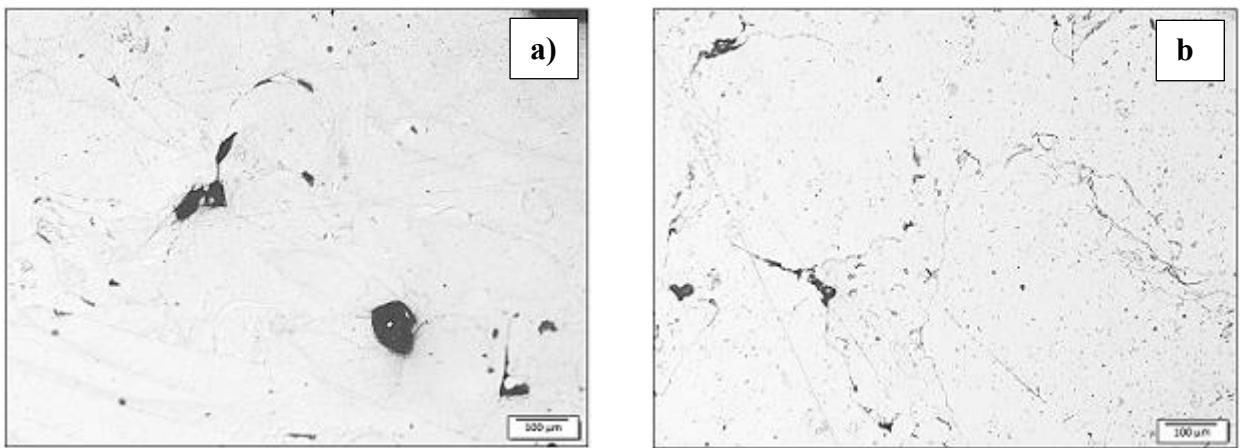
The final experiments, as listed in Table 6, were done to optimize the selective laser melting processing parameters (overlap or hatching space, laser power, and scanning speed) to produce high quality products from 17-4PH stainless steel.

Fig. 14 shows that specimens' numbers 3, 4, 16, and 18 are the optimal specimens, which requires focusing on them and making more comparisons to choose the best. Specimens' numbers 4 and 16 have the highest tensile strength 565 MPa, and 540 MPa, respectively, for yield strength and 945.63 MPa, and 955.68 MPa for ultimate tensile strength as a result of low porosity, as shown in Fig. 15. Specimens' numbers 4, 16, and 18 have the highest relative densities of 97.2%, 95.13%, and 95.28%, respectively. Fig. 16 shows

the stress-strain diagram for specimens' numbers 4 and 16 which have the highest yield and ultimate strength.



**Fig. 14:** a) Relative density, b) yield and ultimate strength for the optimal specimens (final experiments)



**Fig. 15:** The porosity percentage with a magnification of  $100_x$  using different hatching space a) 60 μm and b) 90 μm at a laser power of 200 watts and a scanning speed of 200 mm/sec

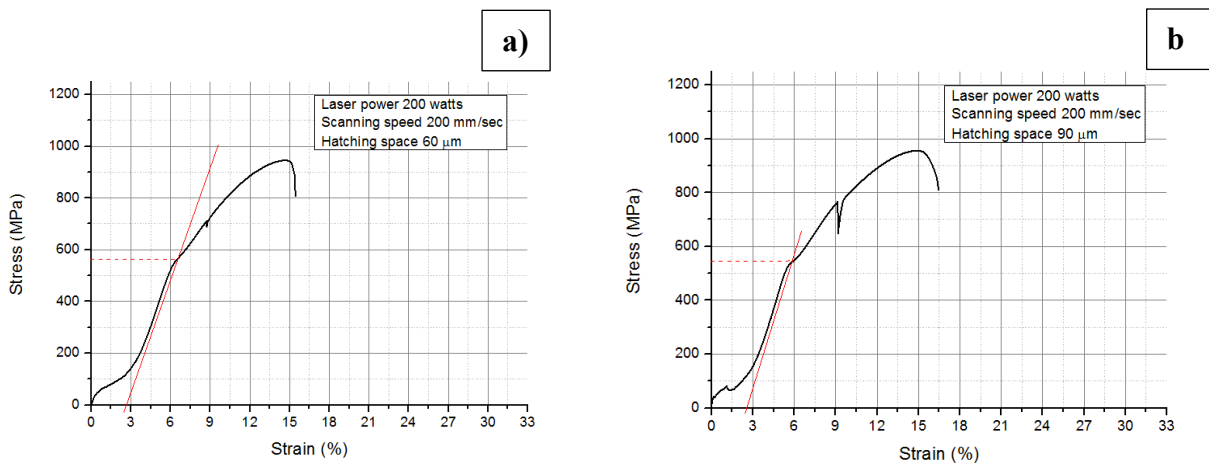


**Fig. 16:** The stress-strain diagram while laser power 200 watts, scanning speed 200 mm/sec and hatching space a) 60 μm b) 90 μm

The micro-hardness of the top and side surfaces of 3, 4, 16, and 18 specimens was measured, and the average values of the ten measured values in each direction are shown in **Table 7**. The results show that the effect of hatching space on micro-hardness is less significant compared with other prevailing parameters such as laser power and scanning speed. Also, it was noticed that the micro-hardness of the side surface is less than the top surface due to the building orientation, as shown in **Fig. 3**. Specimens' numbers 4 and 16 also have the highest micro-hardness, 313.6 HV and 312 HV, respectively, as a result of low porosity, as shown in **Fig. 15**.

**Table 7:** The micro-hardness for top and side surfaces for specimens' number 3, 4, 16 and 18

Specimen No.	$h$ ( $\mu\text{m}$ )	$P$ (Watts)	$v$ (mm/sec)	Micro-hardness (HV)	
				Top surface	Side surface
3	60	150	200	291.6	199.4
4	60	200	200	313.6	273.2
16	90	200	200	312	276.8
18	90	200	400	292.2	266.6

## CONCLUSIONS

Laser power, scanning speed, and hatching space have significant effects on the density, tensile strength, and micro-hardness of SLM-processed 17-4PH stainless steel. The results have shown that high-quality specimens are achieved with increased laser power (at 200 watts) and decreased scanning speed (at 200 mm/sec), with a percentage overlap between 40% and 60%. The results of the study can be summarized as follows:

- The highest density of the SLM-processed specimens is about  $7.53 \text{ g/cm}^3$  which represents about 97.2% of the density of the wrought 17-4PH stainless steel ASTM A693 standard (hot-rolled plates).
- The highest yield strength and ultimate tensile strength that have been obtained are about 565 MPa and 955 MPa, respectively. These values represent about 70% and 95%, respectively, of the mean yield and ultimate strength of the wrought 17-4PH stainless steel ASTM A693 standard (hot-rolled plates). However, the highest elongation that has been obtained is about 15.5%, which is larger than the mean elongation of the wrought 17-4PH stainless steel ASTM A693 standard (hot rolled plates) by about 20%.
- Micro-hardness has also been measured. The highest micro-hardness achieved is about 313.6 HV, which is close to that of the wrought 17-4PH stainless steel ASTM A693 standard (hot-rolled plates).

## ACKNOWLEDGMENTS

I would like to thank the Mechanical Engineering Department, Faculty of Engineering, Al-Azhar University, for their support and encouragement during the research. I would also like to thank the Advanced Digital Manufacturing Department, Manufacturing Institute, CMRDI, for giving me the opportunity to use the lab facilities during my thesis.

## REFERENCES

- [1] Francesca R. Andreacola, Ilaria Capasso, Letizia Pilotti, Giuseppe Brando, " Mechanical performance of 17-4PH stainless steel produced via selective laser melting ", in Conf. Steel and Composite Construction, ce/papers, Portugal, 2022, pp. 196-205.

- [2] Lai-Chang Zhang, Hooyar Attar, " Selective laser melting of titanium alloys and titanium matrix composites for biomedical applications: A review ", *Advanced Engineering materials*, vol. 18, Issue4, pp. 463-475, 2016.
- [3] Thibaut de Terrisa, Olivier Andreau, Patrice Peyre, Frédéric Adamski, Imade Koutiri, Cyril Gorny, Corinne Dupuya, "Optimization and comparison of porosity rate measurement methods of Selective Laser Melted metallic parts", *Elsevier, Additive Manufacturing*, vol 28, 2019, pp. 802-813.
- [4] Liang Huang, Yan Cao, Haiyue Zhao, Yufei Li, Yuanfei Wang, and LiRong Wei, "Effect of process parameters on density and mechanical behaviour of a selective laser melted 17-4PH stainless steel alloy", *Open Physics*, pp. 66-77, 2022.
- [5] P. Ponnusamy, Basant Sharma, S.H. Masood, R.A. Rahman Rashid, Riyan Rashid, S. Palanisamy, D. Ruan, "A study of tensile behavior of SLM processed 17-4 PH stainless steel", *Elsevier, Materials Today : Proceedings*, vol. 45, pp. 4531-4534, 2021.
- [6] P. Ponnusamy, S.H. Masood, D. Ruan, S. Palanisamy, R.A. Rahman Rashid, Omar Ahmed Mohamed, "Mechanical performance of selective laser melted 17-4 PH stainless steel under compressive loading", ", in *Conf. the 28th Annual International Solid Freeform Fabrication Symposium*, 2017, pp. 321-331.
- [7] H. Eskandari, H.R. Lashgari, L. Ye, M. Eizadjou, H. Wang, "Microstructural characterization and mechanical properties of additively manufactured 17–4PH stainless steel", *Elsevier, Materials Today Communications*, vol. 30, 2022.
- [8] Sara Giganto, Susana Martí'nez-Pellitero, Joaquín Barreiro, Paola Le, M<sup>a</sup> Angeles Castro-Sastre, " Impact of the laser scanning strategy on the quality of 17-4PH stainless steel parts manufactured by selective laser melting", *Elsevier, journal of materials research and technology*, vol. 20, pp. 2734-2747, 2022.
- [9] Mohamad Mahmoudi, Alaa Elwany, Aref Yadollahi and Scott M. Thompson, Linkan Bian, Nima Shamsaei, " Mechanical properties and microstructural characterization of selective laser melted 17-4 PH stainless steel ", *Rapid Prototyping Journal*, vol. 23, pp. 280 –294, 2017.
- [10] Aref Yadollahi, Nima Shamsaei, Scott. M. Thompson, Alaa Elwany, Linkan Bian, " Mechanical and microstructural properties of selective laser melted 17-4 PH stainless steel ", in *Conf. of the ASME 2015 International Mechanical Engineering Congress and Exposition*, Houston, Texas, 2015.
- [11] Abiodun Bayode, Esther Titilayo Akinlabi, Sisa Pityana, Mxolisi Brendon Shongwe, "Effect of Scanning Speed on Laser Deposited 17-4PH Stainless Steel", *2017 8th International Conference on Mechanical and Intelligent Manufacturing Technologies (ICMIMT)*, 2017.
- [12] Zhiheng Hu, Haihong Zhu, Hu Zhang, Xiaoyan Zeng, "Experimental investigation on selective laser melting of 17-4PH stainless steel", *Elsevier, Optics & Laser Technology*, vol. 87, pp. 17-25, 2017.
- [13] Paola Leo, Sonia D'Ostuni, Patrizia Perulli, Maria Angeles Castro Sastre, Ana Isabel Fernández-Abia, Joaquin Barreiro, " Analysis of microstructure and defects in 17-4 PH stainless steel sample manufactured by selective laser melting ", in *Conf. 8th Manufacturing Engineering Society*, Madrid, Spain, Elsevier, *Procedia Manufacturing*, vol. 41, 2019, pp. 66–73.
- [14] H.R. Lashgaria, Y. Xue, C. Onggowarsito, C. Kong, S. Li, "Microstructure, tribological properties and corrosion behaviour of additively manufactured 17-4PH stainless steel: effects of scanning pattern, build orientation, and single vs. double scan", *Elsevier, Materials Today Communications*, vol. 25, 2020.